UNIVERSITÀ DEGLI STUDI DI TRIESTE

Bioresorbable vascular scaffold radial expansion and conformation compared to a metallic platform: Insights from in vitro expansion in a coronary artery lesion model

This is the peer reviewed (post-print) version of the following article:

Original
Bioresorbable vascular scaffold radial expansion and conformation compared to a metallic platform: Insights from in vitro expansion in a coronary artery lesion model / Foin, N., Lee, R., Bourantas, C., Mattesini, A., Soh, N., Lim, J.E., Torii, R., Ng, J., Liang, L.H., Caiazzo, G., Fabris, E., Kilic, D., Onuma, Y., Low, A.F., Nijjer, S., Sen, S., Petraco, R., Al Lamee, R., Davies, J.E., Di Mario, C., et al.. - In: EUROINTERVENTION. - ISSN 1774-024X. - 12:7(2016), pp. 834-844. [10.4244/EIJV12I7A138]

Availability:
This version is available at: 11368/2962649 since: 2020-04-21T12:16:03Z
Publisher:

Published
DOI:10.4244/EIJV12I7A138
Terms of use:

Some rights reserved. More details in the PostPrint rights section below.

License:
Digital Rights Management not defined

Publisher copyright

-.-

(Article begins on next page)

19 October 2026

arTs Università degli Studi di Trieste
Archivio della ricerca – postprint

Bioresorbable vascular scaffold radial expansion and conformation compared to a metallic platform: insights from in vitro expansion in a coronary artery lesion model

Nicolas Foin[1]*, MSc, PhD; Renick Lee[1], BEng; Christos Bourantas[2], MD, PhD; Alessio Mattesini[3,4], MD; Nicole Soh[1], BSc; Jie En Lim[1], BSc; Ryo Torii[2], PhD; Jaryl Ng[1], BEng; Leo Hwa Liang[5], PhD; Gianluca Caiazzo[3], MD; Enrico Fabris[3], MD; Dogu Kilic[3], MD; Yoshinobu Onuma[6], MD, PhD; Adrian F. Low[5], MD; Sukh Nijjer[7], MD, PhD; Sayan Sen[7], MD, PhD; Ricardo Petraco[7], MD, PhD; Rasha Al Lamee[7], MD; Justin E. Davies[7], MD, PhD; Carlo Di Mario[3], MD, PhD; Philip Wong[1], MD; Patrick W. Serruys[6], MD, PhD

1. National Heart Centre Singapore and Duke-NUS Medical School, Singapore; 2. University College London, London, United Kingdom; 3. BRU, Royal Brompton NHS Trust and Imperial College London, London, United Kingdom; 4. Department of Heart and Vessels, AOUC Careggi, Florence, Italy; 5. National University Singapore, Singapore; 6. Thoraxcenter, Erasmus MC, Rotterdam, The Netherlands and Imperial College London, London, United Kingdom; 7. International Centre for Circulatory Health, National Heart and Lung Institute, Imperial College London, London, United Kingdom

GUEST EDITOR: Takeshi Kimura, MD, PhD; *Department of Cardiovascular Medicine, Graduate School of Medicine, Kyoto University, Kyoto, Japan*

N. Foin and R. Lee have contributed equally to this manuscript.

KEYWORDS

- bioresorbable vascular scaffold (BVS)
- conformation
- post-dilatation

Abstract

Aims: This study aimed to compare the acute expansion behaviour of a polymer-based bioresorbable scaffold and a second-generation metallic DES platform in a realistic coronary artery lesion model. Experimental mechanical data with conventional methods have so far shown little difference between metallic stents and currently available polymer-based bioresorbable scaffolds (BRS). Nevertheless, differences in acute results have been observed in clinical studies comparing BRS directly with metallic DES platforms.

Methods and results: We examined the expansion behaviour of the bioresorbable vascular scaffold (3.0×18 mm Absorb BVS; Abbott Vascular, Santa Clara, CA, USA) and a metallic DES (3.0×18 mm XIENCE Prime; Abbott Vascular) after expansion at 37°C using identical coronary artery stenosis models (in total 12 experiments were performed). Device expansion was compared during balloon inflation and after deflation using microscopy to allow assessment of plaque recoil. Minimal lumen diameter (MLD) and minimal lumen area (MLA) and stent eccentricity were quantified from optical coherence tomography (OCT) imaging at nominal diameter and after post-dilation at 18 atm. The MLA in the models with BVS deployed was 4.92±0.17 mm² while in the metallic DES it was 5.40±0.13 mm² (p=0.02) at nominal pressure (NP), and 5.41±0.20 and 6.07±0.25 mm² (p=0.02), respectively, after expansion at 18 atm. Stent eccentricity index at the MLA was 0.71±0.02 in BVS compared to 0.81±0.02 in the metal stent at NP (p=0.004), and 0.73±0.03 compared to 0.75±0.02 at 18 atm (p=0.39).

Conclusions: Results obtained in this *in vitro* lesion model were comparable to the results in randomised clinical trials comparing BVS and XIENCE stents *in vivo*. Such models may be useful in future BRS developments to predict their acute response *in vivo* in eccentric lesions.

**Corresponding author: National Heart Centre Singapore and Duke-NUS Medical School Singapore, 5 Hospital Drive, Singapore, 169609, Singapore. E-mail: nicolas.foin@gmail.com*

Introduction

Differences in the acute gain and recoil between the bioresorbable vascular scaffold (BVS) and conventional metallic stents have been observed in clinical studies investigating the efficacy of BVS technology[1-4], including in a recent randomised controlled trial comparing both technologies in a large number of patients[4,5]. Despite extensive differences in material properties, experimental mechanical characterisation with conventional *in vitro* methods has shown little difference in radial support between metallic stents and the currently available polymer-based BVS[6-8] **(Table 1, Table 2)**. To understand the difference in acute expansion results between BVS and a second-generation metallic platform observed *in vivo* in recent randomised studies, we used an *in vitro* compliant model of an asymmetric coronary artery stenosis to compare directly the expansion behaviour of the same commercially available BVS platform and a second-generation metallic platform.

Methods

EXPANSION PROTOCOL

We tested the expansion behaviour of the everolimus-eluting bioresorbable vascular scaffold (3.0×18 mm Absorb BVS; Abbott Vascular, Santa Clara, CA, USA) and an everolimus-eluting metallic DES (3.0×18 mm XIENCE Prime; Abbott Vascular) in an identical coronary artery lesion model. The lesion models were made from silicone (MED-4735 with 35 Shore hardness; NuSil Technology LLC, Carpinteria, CA, USA) with a 0.45 mm wall thickness, a reference diameter of 2.75 mm and a minimal lumen diameter of 1.6 mm, representative of a 40% diameter stenosis lesion (material properties: isotropic-elastic; density 1,110 kg/m^3; Young's modulus 1.2 MPa; Poisson's ratio 0.48). The devices were advanced in the model to cross the lesion and then deployed at their nominal pressure (NP): 7 atm for the BVS (with slow inflation at 1 atm/2 s) and 10 atm for the XIENCE metallic DES. After microscopy and optical coherence tomographic evaluation, the devices were further dilated to 18 atm using their delivery balloon. Three samples in each arm were tested for the two inflation pressures and all experiments were performed in a 37°C water bath. Twelve experiments were performed in total.

MICROSCOPE AND OCT ASSESSMENT

Devices expanded at NP and 18 atm were inspected and measured under microscopy using a stereomicroscope (Leica MZ16A fluorescence stereomicroscope; Leica Microsystems, Wetzlar, Germany). Microscope measurements were taken both during balloon inflation and after removal of the balloon to assess device recoil using the minimal lumen diameter (MLD) at the lesion site. Microscopic measurement of recoil was based on the model deformation as the inner and outer stent strut contours could not be clearly identified under microscopy (estimated approximation of 0.05 mm).

Percentage recoil was defined as: (MLD during balloon inflation – MLD after balloon deflation)/MLD during balloon inflation * 100 **(Figure 1)**.

Table 1. Design characteristics and radial force of a 3.0 mm XIENCE and Absorb BVS.

A	XIENCE stent	BVS scaffold
Material	CoCr (L-605)	PLLA
Strut thickness, total µm	97	157
Drug	Everolimus	Everolimus
Polymer coating	Fluorinated durable polymer	PLLA
Stent to artery ratio (%)	13.3	27
No. of crowns	6	6
No. of connectors	3	3
Coating thickness, µm	7.8	3
Resorption (months)	NA	18-36

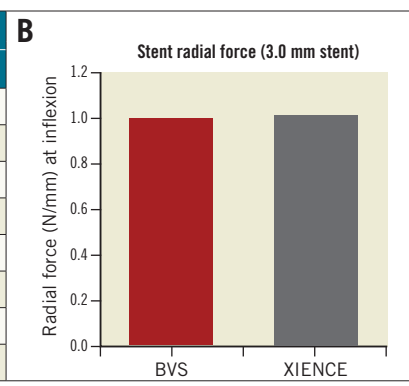

A) Stent design characteristics for XIENCE DES stent and Absorb BVS scaffold (based on 3.0 mm diameter device) (Table 2). B) Conventional iris radial compression test on 3.0 mm BVS and XIENCE sample shows similar radial strength between the BVS and XIENCE platforms (test performed on 3.0×18 mm BVS and XIENCE sample).

Table 2. Material properties for cobalt-chromium metallic alloy and PLLA biodegradable polymers.

Material	Density (g/cm^3)	Young's modulus of elasticity (GPa)	Tensile strength (MPa)	Elongation at break (%)	Biodegradability (months)
Cobalt-chromium (L-605)	9.1	243	>1,000	>50	–
PLLA	1.2-1.4	2.7-4.0*	40-65	6*	18-36
Oriented PLLA	1.2-1.4	2.7-4.0	80-250	>60	18-36

*Note some of the mechanical properties are only indicative of raw material. Metal and polymer mechanical properties can be modified by manufacturing process[7,8].

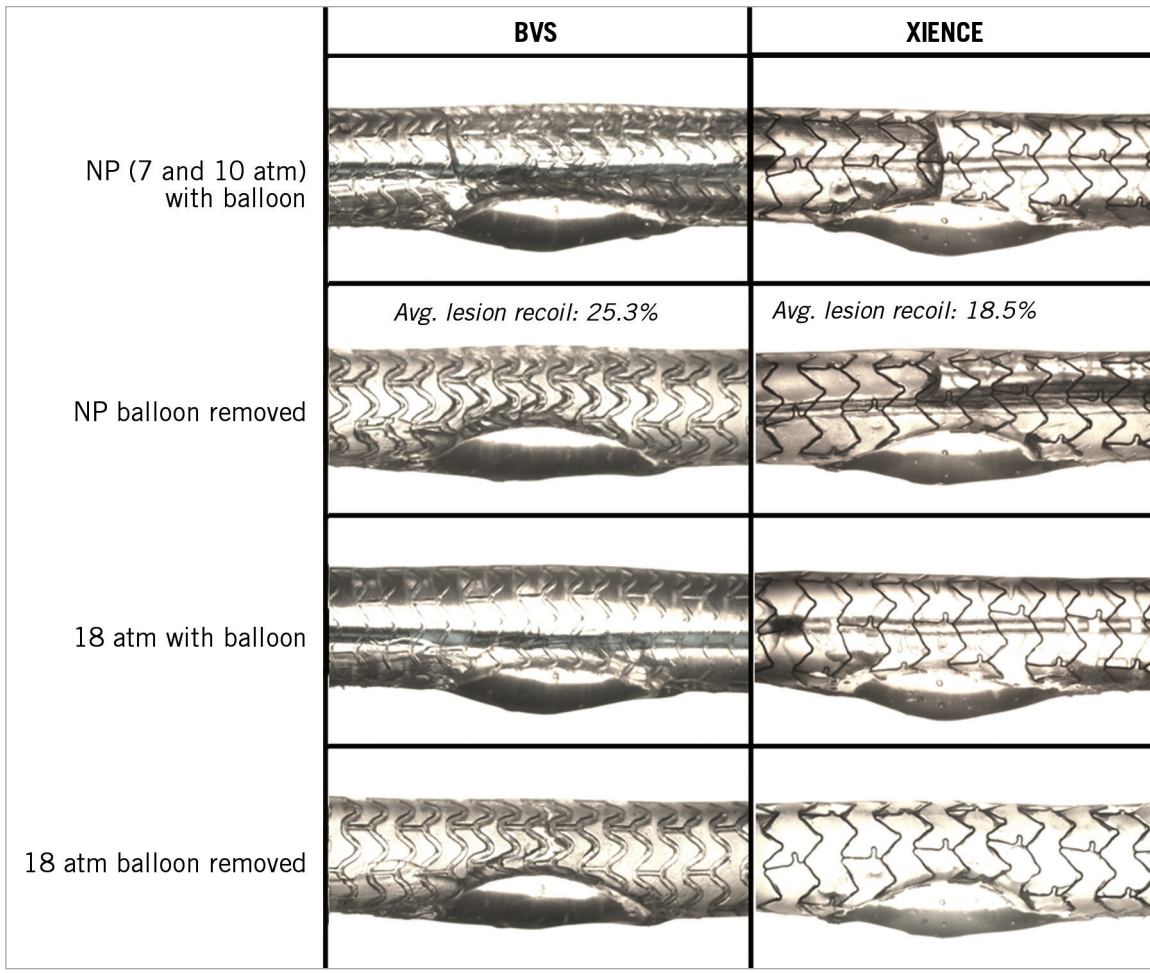

Figure 1. *Representative microscope images of the deployment and difference in post-deployment results between polymer BVS and a metallic XIENCE stent. Both devices were implanted in identical compliant silicone lesion models at nominal pressure (NP=7 atm for BVS and 10 atm for XIENCE) and at 18 atm inflation pressure. Lesion recoil (comparison of stent minimal diameter during and after balloon inflation) is based on the microscope measurements of the MLD (average of 3 experiments).*

The deployed stents/scaffolds were also studied by intraluminal optical coherence tomography (OCT) imaging (C7 with Dragonfly™ OCT catheter; St. Jude Medical, St. Paul, MN, USA). Reference stent diameter (mean diameter at the proximal and distal stent edges), reference stent area, minimal lumen area (MLA: lumen area inside the deployed stent at the frame with the lowest lumen area) and the minimum lumen diameter (MLD) were recorded (ILUMIEN™ OCT software; St. Jude Medical). Eccentricity was calculated as the ratio of the MLD to the maximal diameter (long axis) measured at the MLA. In-stent residual obstruction was calculated as: (reference stent area−MLA)/reference stent area * 100. Percentage of strut malapposition was quantified from the OCT pullbacks at the shoulders of the lesion to assess stent conformation and maximal cross-sectional rate of malapposed struts **(Figure 2, Figure 3)**.

COMPUTATIONAL FLUID DYNAMICS SIMULATION

Idealised two-dimensional (2D) models were created based on 2D midsections representative of the average *in vitro* MLD results after BVS and metallic stent implantation at nominal pressure. The 2D models were constructed and meshed using ANSYS Workbench (ANSYS, Inc., Canonsburg, PA, USA). Meshes were generated with quadrilateral elements and subsequently imported to a commercial computational fluid dynamics (CFD) software, Fluent 15.0 (ANSYS, Inc.), for flow analysis. Blood was assumed to be an incompressible Newtonian fluid and blood material properties were defined as density=1,060 kg/m^3 and dynamic viscosity=0.0035 Pa·s. Flow was also assumed to be laminar. A fully developed steady parabolic velocity profile with peak velocity 0.5 m/s (representative of the flow velocity in the human coronary circulation) was imposed as the inlet boundary condition.

Flow patterns and shear rates were analysed to study relations between expansion behaviour and flow characteristics in lesion models implanted with BVS vs. metallic DES.

FINITE ELEMENT ANALYSIS

We used finite element analysis (FEA) to estimate the change in wall stress after implantation of the BVS and XIENCE at NP and 18 atm.

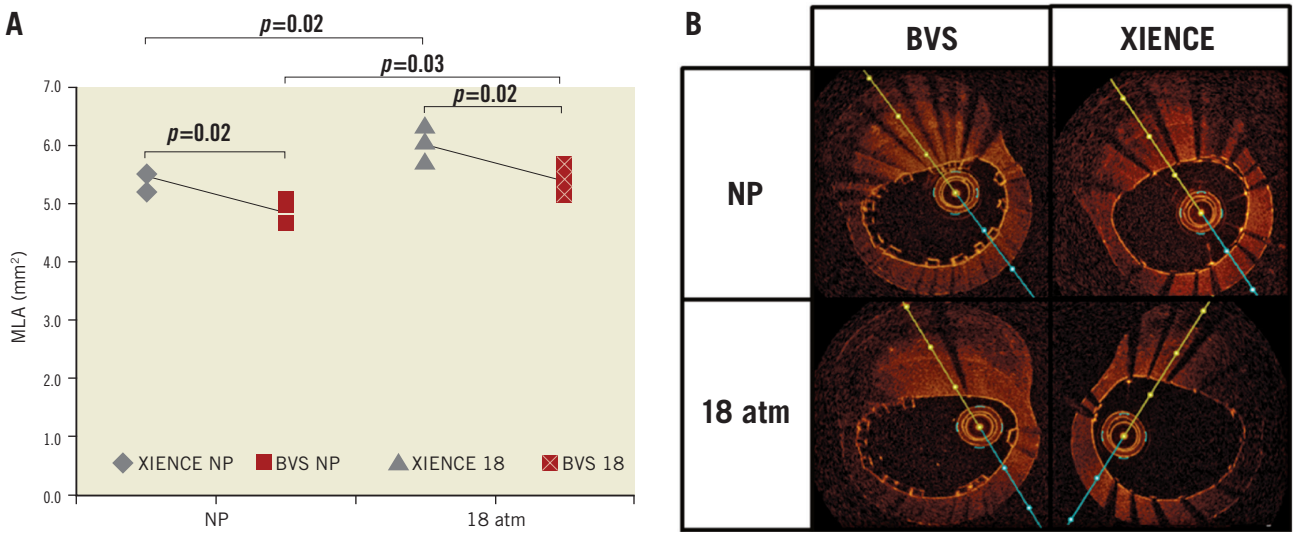

Figure 2. *MLA after 3.0 mm BVS and metallic stent (XIENCE) implantation. A) MLA at NP and 18 atm pressure (repeat of 3 experiments each). B) Representative OCT cross-section at the MLA. NP: nominal pressure; 18 atm: expansion at 18 atm with delivery balloon.*

A 2D model of the midsection of the artery lesion silicone phantom geometry was recreated virtually on computer. The material properties for the silicone MED-4735 were imported (density 1,110 kg/m^3; Young's modulus 1.2 MPa; Poisson's ratio 0.48) in the FEA software. Boundary conditions and a loading condition were imposed, where pressure was exerted normally against

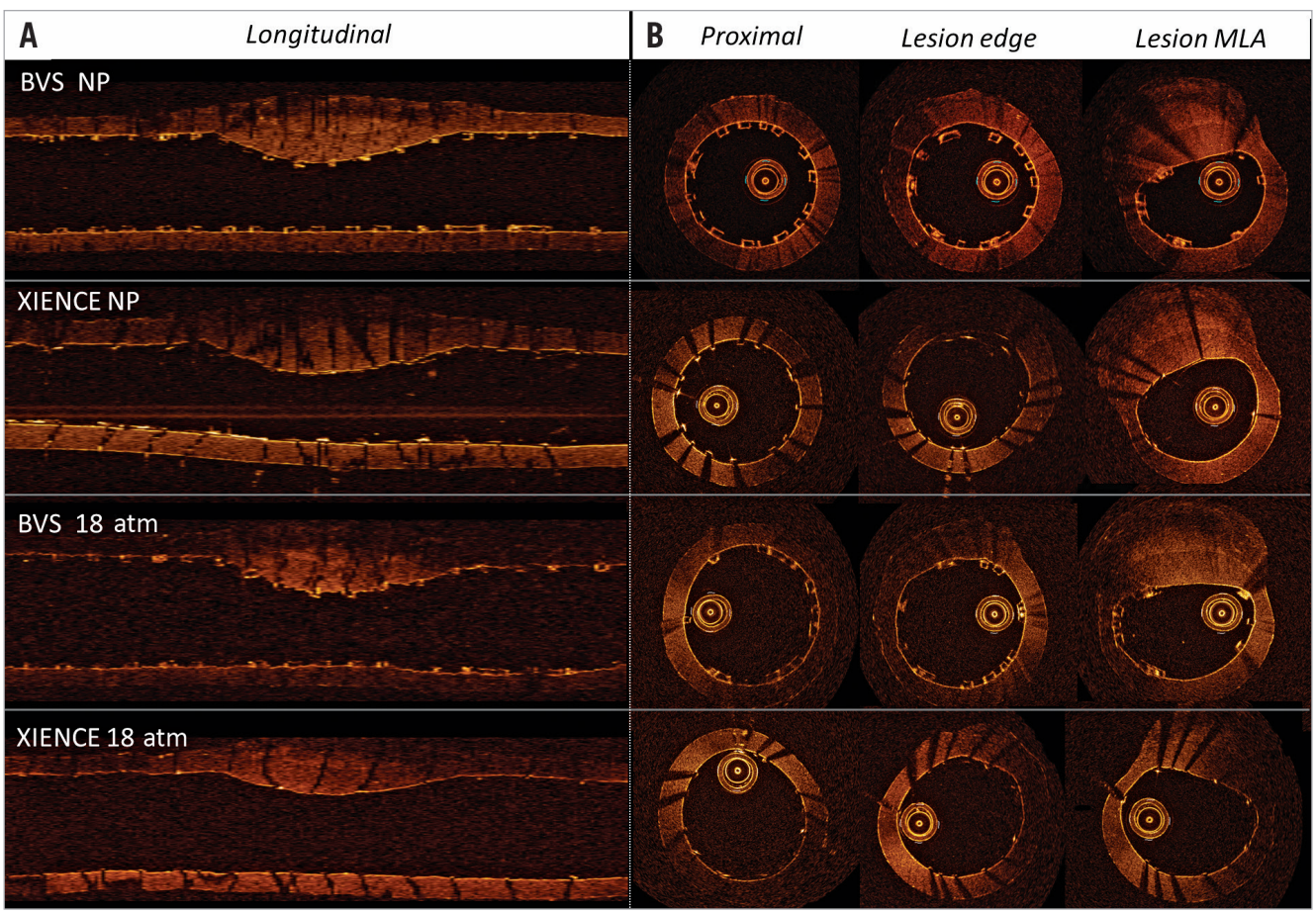

Figure 3. *Model with BVS and metallic stent (XIENCE) implantation at NP and 18 atm pressure. A) Representative longitudinal OCT section. B) Representative OCT cross-sections in proximal stent reference, lesion edge and lesion MLA.*

the inner wall of the 2D model. The model was then meshed into CPS6M elements, six-node modified quadratic plane stress triangles, and submitted for FEA. Simulations were carried out using the commercial FEA software Abaqus 6.13 (Dassault Systèmes, Waltham, MA, USA). Using the method stated above, the load applied in the FEA model was adjusted to match the MLA from the *in vitro* results using an algorithm so that wall stress for particular MLAs could be compared.

STATISTICAL ANALYSIS

OCT measurements were averaged between experiments. The results of the experiments are provided as mean with standard deviation (±SD). Comparisons between measurements were tested by unpaired t-test and Tukey multiple comparisons test (GraphPad Prism; GraphPad Software Inc., La Jolla, CA, USA). A p-value <0.05 was considered as statistically significant.

Results

EXPANSION BEHAVIOUR IN BVS AND METALLIC STENT

OCT measurements before device implantation demonstrated an MLA of 3.75 mm^2. After BVS and metallic DES implantation at NP, MLA increased to 4.92±0.17 mm^2 and 5.40±0.13 mm^2, respectively (difference XIENCE-BVS=0.48 mm^2, p=0.02). The average MLD was 2.07±0.03 mm in the BVS and 2.33±0.05 mm in the XIENCE metal stent at NP, respectively, (p=0.002). Stent eccentricity index after deployment at NP was on average 0.71±0.02 in the BVS group and 0.81±0.02 in the metal stent group (p=0.004).

The reference stent areas measured at NP were similar for BVS and metal stents (on average 6.71±0.22 mm^2 for BVS and 6.78±0.06 mm^2 for the metal stent). Because of the difference in MLA, in-stent percentage residual obstruction was 26.7±0.3% for BVS and 20.4±1.7% in the XIENCE metallic stent at NP (p=0.003) **(Table 3, Figure 2, Figure 4)**.

PLAQUE RECOIL

Percentage recoil at the stenosis site (comparison of stent MLD during and after balloon inflation) was 25.4±8.6% for BVS and 18.5±2.4% for metal stents for nominal deployment (p=0.18) and 37.2±5.6% vs. 23.6±1.6% at 18 atm (p=0.005).

Percentage recoil outside of the lesion was similar in the BVS and metal stent (4.2±1.3% vs. 6.6±2.0% at NP, p=0.13, and 2.3±0.5% vs. 3.3±0.8% at 18 atm, p=0.12) **(Table 4)**.

IMPACT OF DEPLOYMENT PRESSURE

An increase in deployment pressure from NP to 18 atm resulted in a larger MLA in both BVS and metal stents (average MLA was 5.41 mm^2 and 6.07 mm^2, respectively, Δ=0.66 mm^2, p=0.02), resulting in a gain of +0.49 mm^2 for the BVS and +0.67 mm^2 for the metallic stents. In-stent area residual obstruction was 29.8±1.1% in BVS and 15.2±3.6% in metal stents at 18 atm (p=0.003). In-stent area residual obstruction remained unchanged in the BVS (from 26.7% to 29.8%), mainly because of the increase in the scaffold reference area from 6.71±0.22 to 7.70±0.17 mm^2 at 18 atm. Area residual obstruction relative to the vessel reference area was 17.4% in BVS and 9.2% in metal stents at NP (p=0.03) and 9.1% and -2.0% at 18 atm (p=0.04).

The average MLD at 18 atm was 2.23±0.07 mm in the BVS and 2.37±0.06 mm in metal stents, respectively (p=0.06), while the respective gain was 0.58 mm and 0.72 mm compared to the MLD before stent deployment. Interestingly, the eccentricity of

Table 3. Recoil differences between polymer BVS and metallic stent (XIENCE) implanted in identical compliant silicone lesion models.

	NP			18 atm		
	BVS	XIENCE	*p*-value	BVS	XIENCE	*p*-value
Ref. stent diameter (mm)	2.92±0.05	2.94±0.01	0.53	3.13±0.03	3.02±0.02	0.006
MLD (mm)	2.07±0.03	2.33±0.05	0.002	2.23±0.07	2.37±0.06	0.06
MLD strut to strut (mm)	1.73±0.05	2.18±0.04	<0.001	1.87±0.04	2.29±0.05	<0.001
Lumen diameter gain (mm)	0.42±0.05	0.68±0.04	0.002	0.58±0.04	0.72±0.05	0.02
% Diameter stenosis ref. vessel	24.7±1.3	15.3±2.4	0.004	19.0±3.3	13.8±2.9	0.11
Eccentricity index	0.71±0.02	0.81±0.02	0.004	0.73±0.03	0.75±0.02	0.39
Ref. stent area (mm^2)	6.71±0.22	6.78±0.06	0.62	7.70±0.17	7.16±0.09	0.008
MLA (mm^2)	4.92±0.17	5.40±0.13	0.02	5.41±0.20	6.07±0.25	0.02
Lumen area gain (mm)	1.57±0.13	2.05±0.17	0.02	2.06±0.25	2.72±0.20	0.02
% In-stent area residual obstruction	26.7±0.3	20.4±1.7	0.003	29.8±1.1	15.2±3.6	0.003
% Area residual stenosis ref. vessel	17.4±3.4	9.2±2.8	0.03	9.1±4.0	–2.0±5.0	0.04
Max. % strut malapposition at the lesion edge	20.9±4.0	29.1±9.3	0.23	6.3±5.6	6.2±5.4	0.98
% Stent to artery ratio (reference)	33.3±2.2	14.8±2.0	<0.001	27.6±1.9	13.0±0.7	<0.001
% Stent to artery ratio (at lesion)	40.9±1.6	19.8±1.6	<0.001	35.3±0.6	17.2±0.3	<0.001

Twelve different experiments were performed in total and each OCT measurement is provided as an average of three samples±SD.
MLA: minimal lumen area; MLD: minimal lumen diameter

Table 4. Differences between polymer BVS and metallic stent (XIENCE) implanted in identical compliant silicone lesion models.

	NP			18 atm		
	BVS	XIENCE	*p*-value	BVS	XIENCE	*p*-value
% Recoil after balloon deflation (reference)	4.2±1.3	6.6±2.0	0.13	2.3±0.5	3.3±0.8	0.12
% Recoil after balloon deflation (lesion)	25.4±8.6	18.5±2.4	0.18	37.2±5.6	23.6±1.6	0.005

Microscope measurements of recoil (difference during/after balloon inflation). Twelve different experiments were performed in total and each measurement is provided as an average of three samples±SD.

BVS measured at 18 atm was slightly closer to that of metal stents (0.73±0.03 compared to 0.75±0.02) **(Table 3, Figure 2, Figure 4)**.

STRUT CONFORMATION

The maximal cross-sectional rate of malapposed struts measured from OCT at the lesion shoulder was 20.9% in BVS and 29.1% in metal stents at NP (p=0.23). Strut malapposition was observed only at the proximal and distal shoulder of the lesion after nominal pressure deployment. This was largely corrected after post-dilation with re-inflation of the balloon to 18 atm. The rate of strut malapposition at the lesion edge was reduced to 6.3% and 6.2%, respectively, following inflation of the balloon at 18 atm (p=0.98) **(Table 3, Figure 4)**.

Maximal strut to wall malapposition distance observed was similar in both devices: 0.09±0.03 mm in the BVS and 0.11±0.07 mm in the metal stents at NP, reduced to 0.03±0.03 mm and 0.04±0.04 mm at 18 atm.

STENT TO ARTERY RATIO

The parameter was calculated for the devices expanded at the respective pressures in the reference and lesion segments. At the reference, the ratio was 33.3±2.2% for BVS and 14.8±2.0% for XIENCE at nominal pressure and 27.6±1.9% and 13.0±0.7%, respectively, at 18 atm. At the lesion, the ratio was 40.9±1.6% for BVS and 19.8±1.6% for XIENCE at nominal pressure and 35.3±0.6% and 17.2±0.3%, respectively, at 18 atm **(Table 3)**.

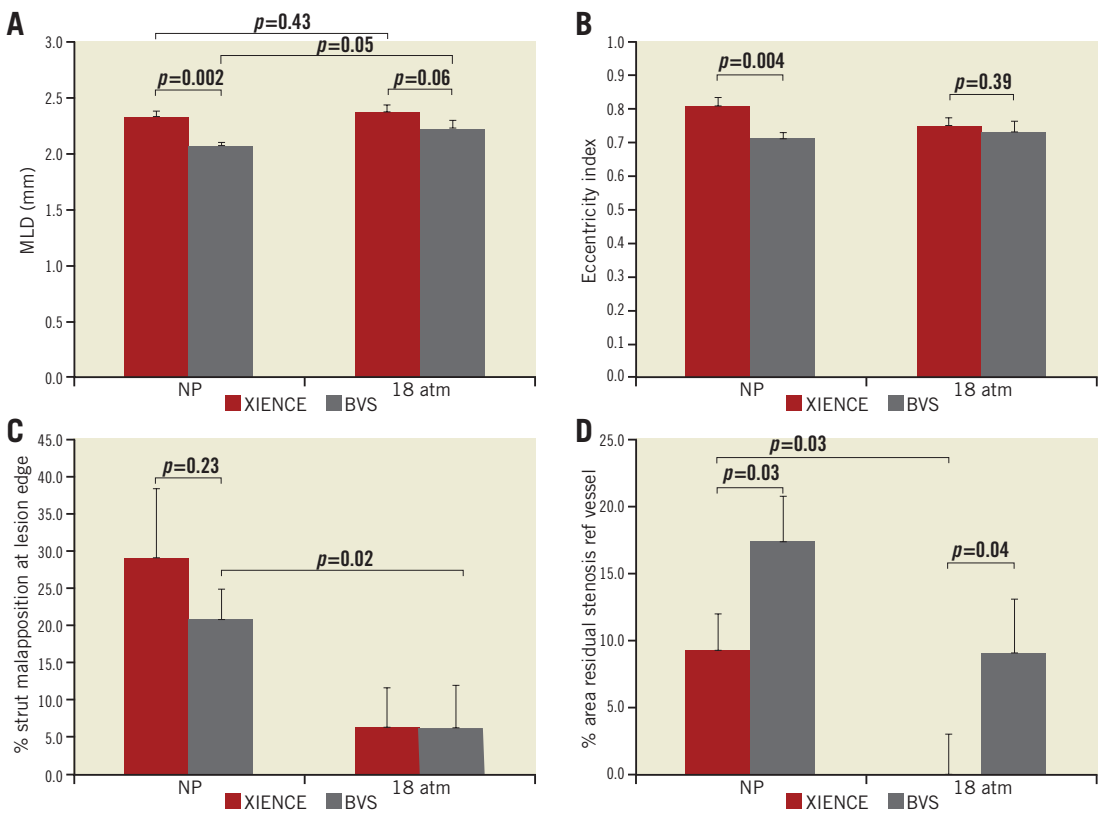

Figure 4. *OCT measurements in the lesion models after 3.0 mm BVS and XIENCE metal stent deployment. A) MLD (miminal lumen diameter). B) Eccentricity index. C) Percentage strut malapposition at the lesion shoulder. D) Percentage area residual stenosis (relative to the reference vessel area). Each result is displayed as mean of three experiments and SD. NP: nominal pressure; 18 atm: expansion at 18 atm with delivery balloon*

COMPUTATIONAL FLUID DYNAMICS

In both models, the highest shear rate values were confined to the edges of the strut. Regions of high shear rate were also observed around the struts, especially in the stenosed region in both models. The higher shear rates observed in the BVS model in the stenosed region are the result of the high velocity stream. In addition, both models exhibited areas of recirculation after the lesion, with the BVS model exhibiting a greater area of recirculation and negative flow velocity. This may be attributed to the smaller strut to strut MLD obtained in the BVS model **(Figure 5)**.

FINITE ELEMENT ANALYSIS

The FEA results show the stress-strain distribution in the lesion model after the implantation of the two different devices, BVS and XIENCE. The results showed that the MLA obtained from the *in vitro* experiments at both pressures translated into different stresses within the vessel wall after BVS compared to XIENCE implantation **(Figure 6)**.

Discussion

SUMMARY

The main insights from this *in vitro* study are the following:

There were noticeable differences in the expansion behaviour of BVS and metal stents in this lesion model:

1. The MLA was smaller in BVS compared to that in metal stents at NP implantation (4.92 and 5.40 mm^2, respectively, p=0.02) and after post-dilation at 18 atm (5.41 and 6.07 mm^2, respectively, p=0.02) **(Table 3, Figure 2)**.
2. Stent eccentricity was more marked in the BVS (lower eccentricity index) as compared with the metallic stent group **(Table 3, Figure 4)**.
3. Although there was no significant difference in recoil between the BVS and metallic stent at the proximal and distal reference segment, there was more plaque recoil at the lesion with the BVS compared to the metallic XIENCE platform, at both NP and 18 atm pressure.
4. Higher inflation pressure (18 atm) led to an increase in measured MLA and MLD and improved strut apposition at the lesion shoulders for both designs **(Table 3, Figure 2, Figure 4)**.

Comparison of the *in vitro* lesion model results showed that such models may predict *in vivo* device behaviour more closely than conventional approaches.

COMPARISON WITH IN VIVO RESULTS: ACUTE GAIN

The Absorb BVS was the first bioresorbable polymer scaffold to be evaluated directly against a second-generation metallic drug-eluting stent in a randomised controlled trial (RCT)[4]. The ABSORB II trial included 501 patients and initial results showed comparable results at one year in terms of safety and efficacy endpoints[4]. The average nominal size of the devices used in this trial was 3.02 mm and the average reference vessel diameter 2.60 mm, similar to those in this *in vitro* experiment. Angiographic results in ABSORB II showed a small but significant difference in acute gain between devices, despite similar lesion characteristics in both groups. Post-procedural MLD in the BVS group was lower than in the metal XIENCE group,

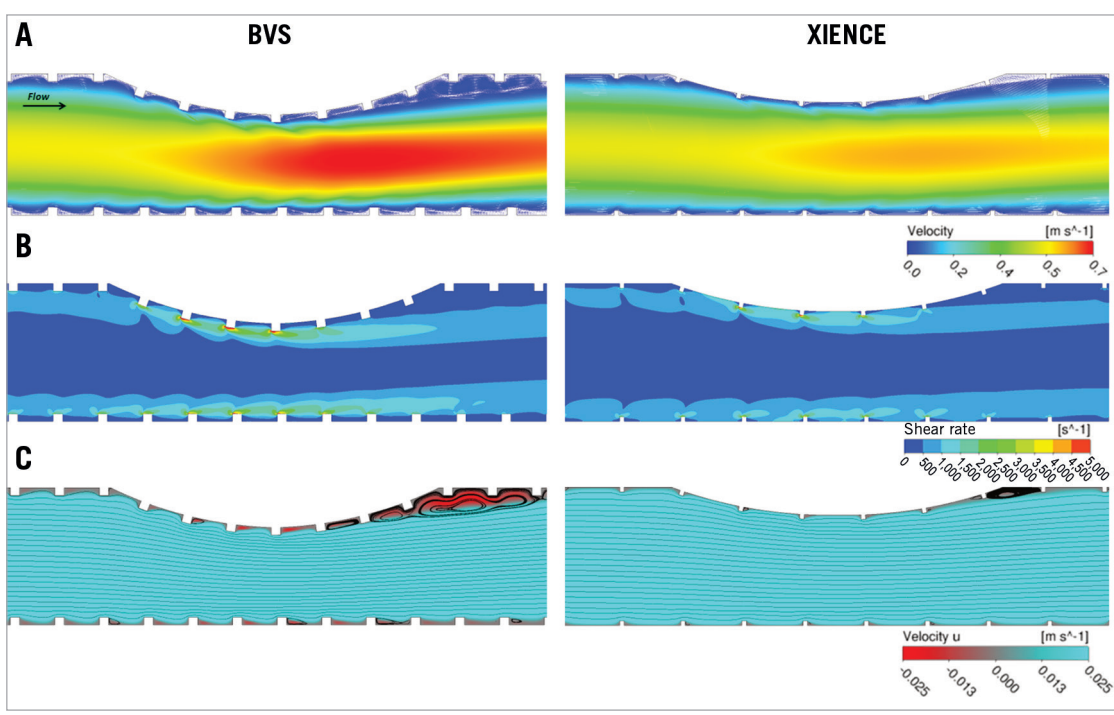

Figure 5. *Computational flow simulations. Flow profiles corresponding to the in vitro results (Figure 3) at nominal pressure after BVS (left panels) and metallic XIENCE stent (right panels) implantation. A) Velocity magnitude. B) Shear rate. C) Streamline plots and recirculation.*

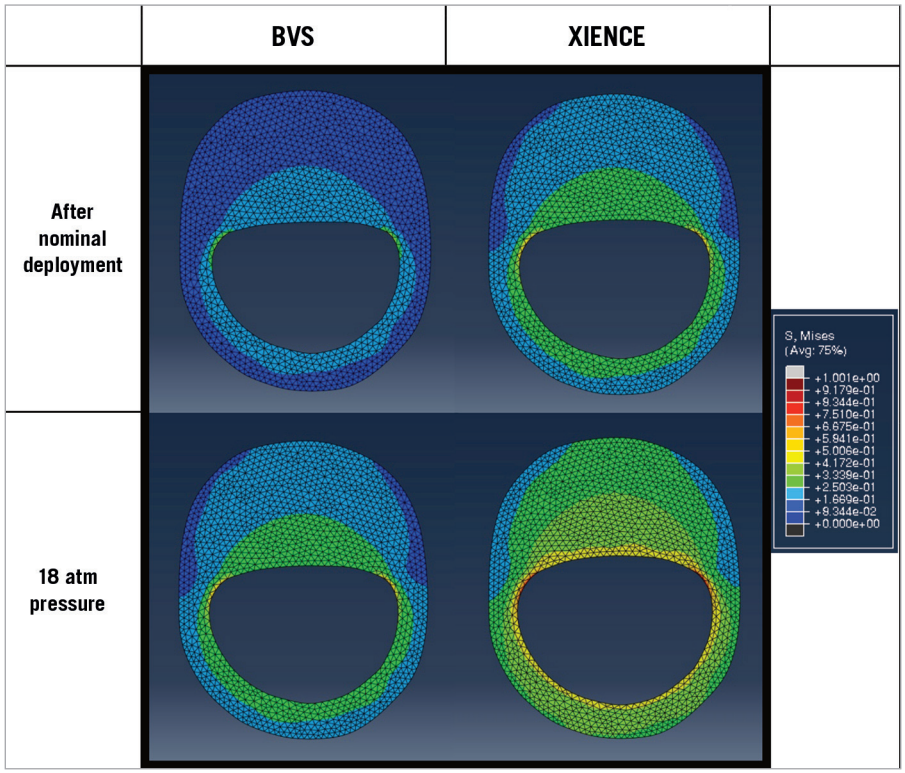

Figure 6. *Wall stress distribution. Contour map of stress distribution in the wall and lesion derived from FEA. Results were calculated to match the MLA from the lesion model experiments of the BVS and XIENCE stent, at the two different pressures (NP and 18 atm). The comparison is indicative of the change in stress-strain values in the artery wall after BVS and metallic stent, respectively.*

(2.22 mm and 2.50 mm on average, respectively, p<0.001)[4]. An earlier pooled patient analysis of the ABSORB cohort B and the SPIRIT II trial demonstrated a similar smaller post-procedural in-stent MLD in the BVS group compared to the XIENCE group (2.27±0.27 mm vs. 2.44±0.26 mm, p=0.02)[3]. Other RCT studies comparing BVS and XIENCE have also recently shown a difference in acute gain between devices: in ABSORB III, post-procedural MLD was 2.37 mm in the BVS group and 2.49 mm in the DES arm (p<0.001)

In our model, the difference in the results observed in terms of final MLD between the devices was remarkably similar to the findings of these *in vivo* studies (MLD: 2.07 mm in the BVS and 2.33 mm in XIENCE at NP and 2.23 mm and 2.37 mm at 18 atm, respectively) **(Table 3, Figure 4)**.

While post-procedural in-device MLD measured by QCA was significantly different in several RCTs comparing BVS and XIENCE, including ABSORB II, ABSORB Japan, ABSORB China and ABSORB III[4,5,9-11], the difference between the two devices was relatively limited (0.16 mm on average), and results were not significantly different in the EVERBIO II trial[12]. One should note that post-procedural QCA measurements with BVS are affected by the large strut thickness of the device excluding contrast from flowing near the true lumen borders, which may underestimate lumen diameter in the device.

There were similar differences in the intraluminal imaging data reported in our study (MLA: 4.92 mm^2 in BVS and 5.40 mm^2 in XIENCE stent at NP; Δ=0.48 mm^2, p=0.02) **(Table 3, Figure 2)** and in the ABSORB II trial imaging data, where the post-procedure MLA was 4.89±1.38 mm^2 and 5.73±1.51 mm^2 for the Absorb BVS and XIENCE stent, respectively (Δ=0.84 mm^2, p<0.001)[4].

COMPARISON WITH IN VIVO RESULTS: RECOIL

We used microscopy to evaluate device recoil during and after balloon deflation *in vitro*. We found no difference in device recoil between the BVS and XIENCE stent at the proximal and distal reference segment (4.2% vs. 6.6% at NP, p=0.13, and 2.3% vs. 3.3% at 18 atm, p=0.12) **(Table 4)**. Quantitative coronary angiography (QCA) assessment of device recoil was comparable[1,2]. In the ABSORB II trial, device overall recoil measured by angiography was 0.19 mm (equivalent to 5.8% for both devices)[4] .

Plaque recoil (recoil after balloon deflation estimated by microscopy at the stent MLD) was, in our experiment, 25.4% for BVS and 18.5% for metal stents at NP (Δ=6.9%) and 37.2% vs. 23.6% at 18 atm (Δ=13.6%) **(Table 4, Figure 2)**. Based on the post-procedure in-stent MLD measured and the expected maximal diameter of the balloon reported in ABSORB II, acute plaque recoil at the MLD *in vivo* was estimated to be 32.5% with the Absorb BVS and 25.4% in the XIENCE stent (Δ=7.1%)[4] .

COMPARISON WITH IN VIVO RESULTS: ECCENTRICITY AND CONFORMATION

Here, the eccentricity index was estimated at the MLA site and was lower in the BVS group than in the XIENCE group at NP (p=0.004). We only calculated the eccentricity index at the MLA as there was only a single asymmetric lesion. This difference was less marked when we post-dilated the two devices at 18 atm (0.73±0.03 for BVS compared to 0.75±0.02 for XIENCE) **(Table 3, Figure 4)**. In the IVUS analysis of Brugaletta et al, the BVS had a significantly lower eccentricity index as compared to the XIENCE V (0.85±0.08 vs. 0.90±0.06; p<0.01)[13]. Importantly, clinical studies often calculate the eccentricity index as an average along the length of the device.

In our analysis, the malapposition rate (at the lesion shoulder) was numerically higher in the metallic platform at NP and we did not observe any differences between the two platforms at 18 atm. Recently, Mattesini et al used OCT to assess acute geometrical differences in the Absorb BVS and the XIENCE DES in complex coronary artery lesions[14]. No difference in eccentricity was observed with aggressive lesion preparation and post-dilatation in the BVS group using an NC balloon at high pressure.

POLYMER VERSUS METALLIC STENT MECHANICAL PROPERTIES

There are major differences in design and material response between metallic stents and BRS[7,8,15]. Biodegradable polymer materials have inherent limitations in their strength and, while manufacturing processes can improve mechanical properties, achieving a radial force comparable to that of a metallic stent is still a challenge and requires a denser structure with larger strut dimensions (at least 150 µm)[2,7,8]. Bench studies have demonstrated that the BVS has comparable total radial strength and similar recoil to metallic platforms when measured using standard methods[6,16] **(Table 1)**.

However, differences have been observed in terms of acute procedural results in the ABSORB II trial and other clinical studies[4,5,9-11,13]. Radial strength for stents is normally assessed *in vitro* using a compressive force applied uniformly around the device. Such standardised testing methods (see international standards ISO 25539 and ASTM F2081 for cardiovascular devices) provide a high level of reproducibility and accuracy which enables comparison to acceptable performance levels across the industry. However, they may not fully represent the deformation and stress occurring in the presence of an eccentric lesion *in vivo*. The model here allows comparison of expansion in a setting which represents more closely a clinical scenario with a device implanted across an asymmetric lesion.

CLINICAL RELEVANCE AND INSIGHTS FOR GUIDANCE OF BVS IMPLANTATION

Randomised clinical evaluation of metallic DES vs. biodegradable Absorb BVS have shown that both devices produce comparable results at one year in terms of safety and efficacy endpoints[4,5]. It is still premature to assess whether the differences in expansion behaviour observed in BVS and metallic devices post procedure may have any long-term clinical impact. Evidence from RCTs suggests that this does not affect clinical outcome significantly, which is reassuring. The model presented here is representative of a fibrotic lesion, which would not respond to predilatation. BVS are increasingly used for the treatment of complex coronary lesions, including rigid fibrous and calcified plaques[14,17,18], and results underline the importance of lesion preparation to achieve an optimal/maximal expansion of the BVS. Optimal lesion preparation is already highly recommended in practice to optimise implantation of BVS, particularly in the presence of calcified/stiff fibrous lesions. Here, we observed a larger stent to artery ratio with BVS compared with the metallic stent, reaching >35% of the lumen surface at the MLA for the BVS **(Table 3)**. A recent analysis by Kawamoto et al comparing BVS with the CYPHER® Sirolimus-eluting Coronary Stent (Cordis, Johnson & Johnson, Warren, NJ, USA) (similar strut thickness, but approximately half the stent-to-artery ratio of BVS) suggested that a higher footprint may contribute to an increase in the rates of periprocedural myocardial infarction[19].

The importance of post-dilatation to optimise stent expansion has been evidenced in the metallic stent era, and post-procedural MLA has been shown to be a predictor of both restenosis and stent thrombosis[20-23]. Several reports have recently warned about the clinical implications of device underexpansion and the risk of incomplete stent apposition (ISA) in BVS.

Here we observed a significant improvement in MLA, eccentricity and strut apposition after dilation to 18 atm. Furthermore, by staying within the recommendation of dilatation <0.5 mm above scaffold size, we did not observe any scaffold discontinuities at 18 atm in the BVS samples. Initially, post-dilatation was less frequently performed in BVS because of concern over the risk of strut discontinuity. However, post-dilatation was later shown to be safe up to 0.5 mm above scaffold size. A recent meta-analysis of the four recent ABSORB trials in 3,389 randomised patients[11] showed that post-dilatation was actually performed more often in the BVS group compared with the CoCr EES group (66.2% vs. 55.3%, p<0.0001).

Optimisation of BVS is possibly even more important than it is in metal stents because of the higher strut thickness which can affect the local haemodynamics, creating recirculation zones and flow disturbances that increase the risk for thrombosis[24]. Post-dilatation of BVS, within a 0.5 mm limit above scaffold size, is generally recommended nowadays to maximise expansion, minimise ISA and improve BVS strut embedding[14-16,25,26].

Study limitations

The results from this study must be interpreted with caution as *in vitro* experiments in models only provide an approximate representation of the real expansion behaviour of the devices in a diseased coronary artery vessel *in vivo*.

The aim of this study was to present an *in vitro* model that can be used as a complement to conventional preclinical bench testing methods such as radial force iris testing in the development

of future stent/scaffold platforms. Our analysis was limited to the case of a fibrotic elastic lesion and we did not investigate the effect of further lesion preparation with a cutting balloon or rotablator, as these would have damaged the models.

Conclusion

The aim of this study was to present an *in vitro* model that can be used as a complement to conventional mechanical testing methods to evaluate the difference in expansion response in BRS and metallic stent platforms. Experiment results provide insights to identify attributes that impact on BRS deployment results. Such *in vitro* models may be needed in future developments to understand the expected mechanical response of future BRS platforms compared to metallic stents *in vivo*.

Impact on daily practice

Differences in acute expansion can be observed in clinical studies comparing bioresorbable scaffolds (BRS) directly to metallic DES platforms. This study aimed to compare experimentally the acute expansion behaviour of a polymer-based BRS and a second-generation metallic DES platform in a coronary lesion *in vitro* model. Results provide insights to understand the differences in acute deployment behaviour between metallic DES and BRS *in vivo*, particularly in case of a suboptimally prepared lesion. Such *in vitro* experimental results model the expected mechanical response of the BRS platform *in vivo*, and may help us to understand and prevent foreseeable BRS underexpansion.

Guest Editor

This paper was guest edited by Takeshi Kimura, MD, PhD; Department of Cardiovascular Medicine, Graduate School of Medicine, Kyoto University, Kyoto, Japan.

Acknowledgements

The authors would like to thank Dr R. Rapoza for his review of the manuscript.

Conflict of interest statement

This *in vitro* study was initiated and conducted independently by the authors. P.W. Serruys and Y. Onuma are members of the Advisory Board for Abbott Vascular. The other authors have no conflicts of interest to declare. The Guest Editor has no conflicts of interest to declare.

References

1. Tanimoto S, Serruys PW, Thuesen L, Dudek D, de Bruyne B, Chevalier B, Ormiston JA. Comparison of in vivo acute stent recoil between the bioabsorbable everolimus-eluting coronary stent and the everolimus-eluting cobalt chromium coronary stent: insights from the ABSORB and SPIRIT trials. *Catheter Cardiovasc Interv.* 2007;70:515-23.

2. Onuma Y, Serruys PW, Gomez J, de Bruyne B, Dudek D, Thuesen L, Smits P, Chevalier B, McClean D, Koolen J, Windecker S, Whitbourn R, Meredith I, Garcia-Garcia H, Ormiston JA; ABSORB Cohort A and B investigators. Comparison of in vivo acute stent recoil between the bioresorbable everolimus-eluting coronary scaffolds (revision 1.0 and 1.1) and the metallic everolimus-eluting stent. *Catheter Cardiovasc Interv.* 2011;78:3-12.

3. Zhang YJ, Bourantas CV, Muramatsu T, Iqbal J, Farooq V, Diletti R, Campos CA, Onuma Y, Garcia-Garcia HM, Serruys PW. Comparison of acute gain and late lumen loss after PCI with bioresorbable vascular scaffolds versus everolimus-eluting stents: an exploratory observational study prior to a randomised trial. *EuroIntervention.* 2014;10:672-80.

4. Serruys PW, Chevalier B, Dudek D, Cequier A, Carrié D, Iniguez A, Dominici M, van der Schaaf RJ, Haude M, Wasungu L, Veldhof S, Peng L, Staehr P, Grundeken MJ, Ishibashi Y, Garcia-Garcia HM, Onuma Y. A bioresorbable everolimus-eluting scaffold versus a metallic everolimus-eluting stent for ischaemic heart disease caused by de-novo native coronary artery lesions (ABSORB II): an interim 1-year analysis of clinical and procedural secondary outcomes from a randomised controlled trial. *Lancet.* 2015;385:43-54.

5. Ellis SG, Kereiakes DJ, Metzger DC, Caputo RP, Rizik DG, Teirstein PS, Litt MR, Kini A, Kabour A, Marx SO, Popma JJ, McGreevy R, Zhang Z, Simonton C, Stone GW; ABSORB III Investigators. Everolimus-Eluting Bioresorbable Scaffolds for Coronary Artery Disease. *N Engl J Med.* 2015;373:1905-15.

6. Oberhauser JP, Hossainy S, Rapoza RJ. Design principles and performance of bioresorbable polymeric vascular scaffolds. *EuroIntervention.* 2009;5 Suppl F:F15-22.

7. Onuma Y, Serruys PW. Bioresorbable scaffold: the advent of a new era in percutaneous coronary and peripheral revascularization? *Circulation.* 2011;123:779-97.

8. Foin N, Lee RD, Torii R, Guitierrez-Chico JL, Mattesini A, Nijjer S, Sen S, Petraco R, Davies JE, Di Mario C, Joner M, Virmani R, Wong P. Impact of stent strut design in metallic stents and biodegradable scaffolds. *Int J Cardiol.* 2014;177:800-8.

9. Gao R, Yang Y, Han Y, Huo Y, Chen J, Yu B, Su X, Li L, Kuo HC, Ying SW, Cheong WF, Zhang Y, Su X, Xu B, Popma JJ, Stone GW; ABSORB China Investigators. Bioresorbable Vascular Scaffolds Versus Metallic Stents in Patients with Coronary Artery Disease: ABSORB China trial. *J Am Coll Cardiol.* 2015;66:2298-309.

10. Kimura T, Kozuma K, Tanabe K, Nakamura S, Yamane M, Muramatsu T, Saito S, Yajima J, Hagiwara N, Mitsudo K, Popma JJ, Serruys PW, Onuma Y, Ying S, Cao S, Staehr P, Cheong WF, Kusano H, Stone GW; ABSORB Japan Investigators. A randomized trial evaluating everolimus-eluting Absorb bioresorbable scaffolds vs. everolimus-eluting metallic stents in patients with coronary artery disease: ABSORB Japan. *Eur Heart J.* 2015;36:3332-42.

11. Stone GW, Gao R, Kimura T, Kereiakes DJ, Ellis SG, Onuma Y, Cheong WF, Jones-McMeans J, Su X, Zhang Z,

Serruys PW. 1-year outcomes with the Absorb bioresorbable scaffold in patients with coronary artery disease: a patient-level, pooled meta-analysis. *Lancet.* 2016;387:1277-89.

12. Puricel S, Arroyo D, Corpataux N, Baeriswyl G, Lehmann S, Kallinikou Z, Muller O, Allard L, Stauffer JC, Togni M, Goy JJ, Cook S. Comparison of everolimus- and biolimus-eluting coronary stents with everolimus-eluting bioresorbable vascular scaffolds. *J Am Coll Cardiol.* 2015;65:791-801.

13. Brugaletta S, Gomez-Lara J, Diletti R, Farooq V, van Geuns RJ, de Bruyne B, Dudek D, Garcia-Garcia HM, Ormiston JA, Serruys PW. Comparison of in vivo eccentricity and symmetry indices between metallic stents and bioresorbable vascular scaffolds: insights from the ABSORB and SPIRIT trials. *Catheter Cardiovasc Interv.* 2012;79:219-28.

14. Mattesini A, Secco GG, Dall'Ara G, Ghione M, Rama-Merchan JC, Lupi A, Viceconte N, Lindsay AC, De Silva R, Foin N, Naganuma T, Valente S, Colombo A, Di Mario C. ABSORB biodegradable stents versus second-generation metal stents: a comparison study of 100 complex lesions treated under OCT guidance. *JACC Cardiovasc Interv.* 2014;7:741-50.

15. Bourantas CV, Onuma Y, Farooq V, Zhang Y, Garcia-Garcia HM, Serruys PW. Bioresorbable scaffolds: current knowledge, potentialities and limitations experienced during their first clinical applications. *Int J Cardiol.* 2013;167:11-21.

16. Ormiston JA, Webber B, Ben Ubod B, Darremont O, Webster MW. An independent bench comparison of two bioresorbable drug-eluting coronary scaffolds (Absorb and DESolve) with a durable metallic drug-eluting stent (ML8/Xpedition). *EuroIntervention.* 2015;11:60-7.

17. Capodanno D, Gori T, Nef H, Latib A, Mehilli J, Lesiak M, Caramanno G, Naber C, Di Mario C, Colombo A, Capranzano P, Wiebe J, Araszkiewicz A, Geraci S, Pyxaras S, Mattesini A, Naganuma T, Münzel T, Tamburino C. Percutaneous coronary intervention with everolimus-eluting bioresorbable vascular scaffolds in routine clinical practice: early and midterm outcomes from the European multicentre GHOST-EU registry. *EuroIntervention.* 2014;10:1144-53.

18. Ishibashi Y, Onuma Y, Muramatsu T, Nakatani S, Iqbal J, Garcia-Garcia HM, Bartorelli AL, Whitbourn R, Abizaid A, Serruys PW; ABSORB EXTEND Investigators. Lessons learned from acute and late scaffold failures in the ABSORB EXTEND trial. *EuroIntervention.* 2014;10:449-57.

19. Kawamoto H, Panoulas VF, Sato K, Miyazaki T, Naganuma T, Sticchi A, Figini F, Latib A, Chieffo A, Carlino M, Montorfano M, Colombo A. Impact of Strut Width in Periprocedural Myocardial Infarction: A Propensity-Matched Comparison Between Bioresorbable Scaffolds and the First-Generation Sirolimus-Eluting Stent. *JACC Cardiovasc Interv.* 2015;8:900-9.

20. Gerber RT, Latib A, Ielasi A, Cosgrave J, Qasim A, Airoldi F, Chieffo A, Montorfano M, Carlino M, Michev I, Tobis J, Colombo A. Defining a new standard for IVUS optimized drug eluting stent implantation: the PRAVIO study. *Catheter Cardiovasc Interv.* 2009;74:348-56.

21. Doi H, Maehara A, Mintz GS, Yu A, Wang H, Mandinov L, Popma JJ, Ellis SG, Grube E, Dawkins KD, Weissman NJ, Turco MA, Ormiston JA, Stone GW. Impact of post-intervention minimal stent area on 9-month follow-up patency of paclitaxel-eluting stents: an integrated intravascular ultrasound analysis from the TAXUS IV, V, and VI and TAXUS ATLAS Workhorse, Long Lesion, and Direct Stent Trials. *JACC Cardiovasc Interv.* 2009;2:1269-75.

22. Cook S, Wenaweser P, Togni M, Billinger M, Morger C, Seiler C, Vogel R, Hess O, Meier B, Windecker S. Incomplete stent apposition and very late stent thrombosis after drug-eluting stent implantation. *Circulation.* 2007;115:2426-34.

23. Foin N, Gutiérrez-Chico JL, Nakatani S, Torii R, Bourantas CV, Sen S, Nijjer S, Petraco R, Kousera C, Ghione M, Onuma Y, Garcia-Garcia HM, Francis DP, Wong P, Di Mario C, Davies JE, Serruys PW. Incomplete stent apposition causes high shear flow disturbances and delay in neointimal coverage as a function of strut to wall detachment distance: implications for the management of incomplete stent apposition. *Circ Cardiovasc Interv.* 2014;7:180-9.

24. Foin N, Torii R, Mattesini A, Wong P, Di Mario C. Biodegradable vascular scaffold: is optimal expansion the key to minimising flow disturbances and risk of adverse events? *EuroIntervention.* 2015;10:1139-42.

25. De Ribamar Costa J Jr, Abizaid A, Bartorelli AL, Whitbourn R, van Geuns RJ, Chevalier B, Perin M, Seth A, Botelho R, Serruys PW; ABSORB EXTEND Investigators. Impact of post-dilation on the acute and one-year clinical outcomes of a large cohort of patients treated solely with the Absorb Bioresorbable Vascular Scaffold. *EuroIntervention.* 2015;11:141-8.

26. Bourantas CV, Papafaklis MI, Kotsia A, Farooq V, Muramatsu T, Gomez-Lara J, Zhang YJ, Iqbal J, Kalatzis FG, Naka KK, Fotiadis DI, Dorange C, Wang J, Rapoza R, Garcia-Garcia HM, Onuma Y, Michalis LK, Serruys PW. Effect of the endothelial shear stress patterns on neointimal proliferation following drug-eluting bioresorbable vascular scaffold implantation: an optical coherence tomography study. *JACC Cardiovasc Interv.* 2014;7:315-24.